The Journal of Microbiology, September 2001, p.149-153
Vol. 39, No. 3

MINIREVIEW

Regulation Mechanism of Redox Reaction in Rubredoxin

Tongpil Min[1], Marly K. Eidsness[2], Toshiko Ichiye[1], and ChulHee Kang[1]*

[1]*School of Molecular Biosciences, Washington State University, Pullman, WA 99164-4660, USA*
[2]*Department of Chemistry and BioXpress Laboratory, University of Georgia, Athens, GA 30602-2556, USA*

(Received July 30, 2001)

The electron transfer reaction is one of the most essential processes of life. Not only does it provide the means of transforming solar and chemical energy into a utilizable form for all living organisms, it also extends into a range of metabolic processes that support the life of a cell. Thus, it is of great interest to understand the physical basis of the rates and reduction potentials of these reactions. To identify the major determinants of reduction potentials in redox proteins, we have chosen the simplest electron transfer protein, rubredoxin, a small (52-54 residue) iron-sulfur protein family, widely distributed in bacteria and archaea. Rubredoxins can be grouped into two classes based on the correlation of their reduction potentials with the identity of residue 44; those with Ala44 (ex: *Pyrococcus furiosus*) have reduction potentials that are ~50 mV higher than those with Val44 (ex: *Clostridium pasteurianum*). Based on the crystal structures of rubredoxins from *C. pasteurianum* and *P. furiosus*, we propose the identity of residue 44 alone determines the reduction potential by the orientation of the electric dipole moment of the peptide bond between 43 and 44. Based on 1.5 Å resolution crystal structures and molecular dynamics simulations of oxidized and reduced rubredoxins from *C. pasteurianum*, the structural rearrangements upon reduction suggest specific mechanisms by which electron transfer reactions of rubredoxin should be facilitated.

Key words: electron transfer, rubredoxin, redox potential, iron-sulfer

A considerable body of work has elucidated many aspects of the electron transfer processes in biological systems (9, 11, 12, 17, 19). Biological electron transfer is an efficient process even though the physical distances between the participating redox moieties are often quite large. The driving force for transferring these electrons from a donor to an acceptor is determined by the magnitude and the sign of the reduction potential. In biological processes, redox proteins are the keys to controlling the rate and the direction of this electron transfer reaction. The structural relaxation of the redox protein that occurs upon change in the redox state gives rise to the reorganizational energy, which is important in the rates and the reduction potentials.

Electron transfer proteins can modulate the reduction potential of their redox sites, with differences of up to a few hundred mV between homologous proteins with the same redox site and even larger differences between non-homologous proteins with the same redox site (4). To date, however, the basic mechanisms of establishing and controlling the redox potentials of redox proteins are largely unknown and remain the subject of intense research. Comparisons of global protein structures do not yet allow us to predict reduction potential differences among proteins. Determinants of reduction potentials are believed to come from the local structure that surrounds the redox center (8). In order to elucidate these fine structural features, atomic resolution data are absolutely required. Clear understanding of these bioenergetics of the redox proteins will open new prospectives for all biotransformations (carbon fixation, nitrogen fixation, metanogenesis, etc.) and for engineering a variety of biosensors.

The iron-sulfur [Fe-S] proteins are the most widely distributed electron transfer proteins that participate in various biological reactions, and are ubiquitous in living matter (2, 3, 4, 7, 14, 21, 22). Rubredoxin (Rd) with formal redox couples of Fe(III) and Fe(II), is the simplest iron-sulfur redox protein and is found in bacteria and archaea (2, 20). It is known to participate in electron transfer reactions in sulfur, nitrate, and superoxide reduction (7, 10, 13, 22, 23). In addition, Rd from *Desulfovibrio gigas*

* To whom correspondence should be addressed.
(Tel) 1-509-335-1409; (Fax) 1-509-335-9688
(E-mail) chkang@wsunix.wsu.edu

has been shown to be the redox partner of Rd-oxygen oxidoreductase (ROD), the terminal component of a soluble electron transfer chain that couples NADH oxidation to oxygen consumption (10, 21). In *Pseudomonas oleovorans*, Rd is part of a three component system: alkane hydroxylase, Rd, and Rd reductase that carry out the oxidation of alkanes to alkanols (7).

Rubredoxin consists of a short polypeptide chain (52-54 amino acid residues) and its redox site contains a single iron atom, which is tetrahedrally coordinated by four cysteinyl thiolates. The relative simplicity and wealth of available data make rubredoxin a powerful model system for investigating the fundamental molecular behavior of proteins. Four subtle points make Rd a particularly good choice for systematically investigating the various features responsible for tuning the reduction potential and the electron transfer properties. The first is that unlike the hemes, the redox sites of Rds are all relatively small so that the area of direct interactions with the protein is much smaller than that of heme proteins. The second is that the reduction potentials of Rds cover a range of reduction potential (from -60 to 40 mV vs. NHE) (4), even though they all have high similarity in their backbone structure (Fig. 1) and about 50 to 60% sequence identity. The third is that all structurally characterized Rds share an essentially isostructural $[Fe(S_{Cys})_4]$ site, so focus can be placed on the environment, whereas there is much more variability in the metal ligand structure in the copper proteins (1). The fourth point is that it has been very successful in making well-diffracting crystals of various Rd constructs. In general, the sensitivity of crystallization to even single site mutations plus the inherent difficulties associated with obtaining crystals of different oxidation states generally tends to make in-depth study using crystallography a very hard approach. In contrast, we can design Rd recombinants of various redox phenotypes and investigate those at an ultra-fine scale.

Modulation of the reduction potential of rubredoxin

Based on the observation of nine homologous Rds on which we have information about their sequences and reduction potentials, it has been pointed out that Rds may be separated into two classes on the basis of the correlation of their reduction potentials with the identity of residue 44 (24). Those with Ala44 have a redox potential of ~0 mV, and those with Val44 have a redox potential of about 50 mV. A structural determinant causing this -50 mV shift in reduction potential between two different groups of rubredoxins has been predicted by computational studies (24).

In order to confirm this prediction, two Rds from *Pyrococcus furiosus* (Pf) and *Clostridium pasteurianum* (Cp), representing each group, have been mutated at residue 44. The resulting redox potentials of these [V44A]Cp Rd and [A44V]Pf Rd, were measured and the crystal structure of [V44A]Cp Rd was solved (8). In fact, measurements show that [V44A]Cp Rd has a raised reduction potential similar to that of wild type Pf Rd and that [A44V]Pf Rd

Fig. 1. Rubredoxin backbone structure. Rd structure includes a three-stranded-anti-parallel β-sheet and two short α-helices. Sγ (Cys) and Fe are depicted yellow and gray respectively.

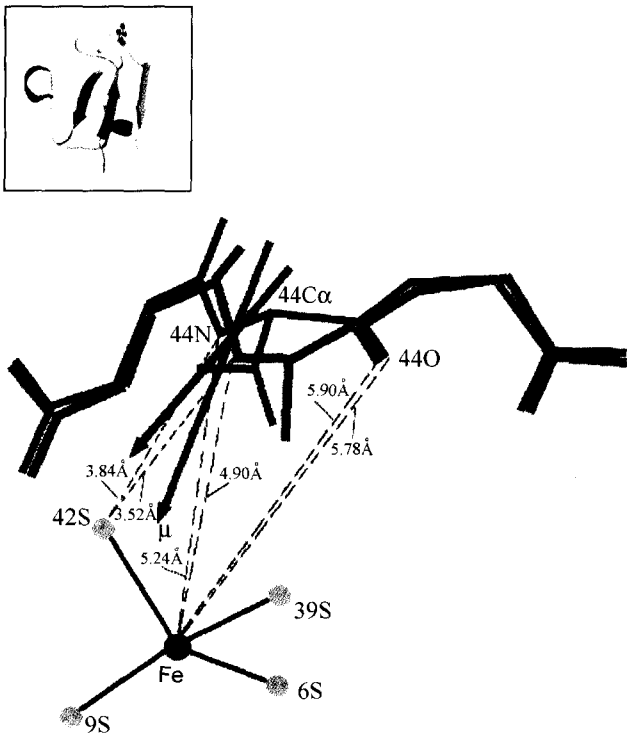

Fig. 2. Top: Rd backbone showing the position of residue Val44. Bottom: comparison of distances from the iron center to the peptide backbone of Val44 and from Cys42 sulfur to Val44 amide nitrogen in wild type CpRd (red) and [V44A]Cp Rd (blue), and the resulting peptide dipole moments.

has a lower reduction potential similar to that of wild type Cp Rd. The 1.6 Å resolution crystal structure shows that the basic coordination geometry of the Fe-S site, including the second sphere NH-S type hydrogen bonding pattern of the ligand residues, is essentially unaffected by the V44A mutation. However, significant structural changes at residue 44 were found in both structures (Fig. 2). The distance between the Ala44 peptide nitrogen atoms and the Fe centers is 4.9 Å, which is significantly shorter than the corresponding (Val44)-NH-Fe distances in the wild type Cp Rd crystal structure. The V44A mutation in Cp Rd also shortens the hydrogen bond distance between the residue 44 peptide nitrogen and the Cys42-sulfur by an average of 0.32 Å compared to that of wild type Cp Rd (3.84 Å). In short, a single mutation (Val to Ala) at position 44 of Cp Rd makes a local environment at residue 44 and a reduction potential very similar to those of Pf Rd. These results support that the identity of residue 44 and its consequent peptide electric dipole moment alone determines whether Rd reduction potential of about -50 or 0 mV is observed. For our [V44A] and [A44V] Rds, other contributions in addition to the movement of the peptide dipole would seem to be relatively minor. Increased exposure of the Fe-S site to solvent water accompanying the Val-Ala substitution seems unlikely, given how well the Ala methyl group in [V44A]Cp Rd occupies the space previously occupied by the Val side chain.

Comparison of oxidized and reduced structures of rubredoxin

There have been several attempts to analyze the crystal structures of the oxidized and reduced forms of the same redox protein to understand the underlying structural features responsible for their redox reactions. These studies were mainly achieved by the approach that crystal structures of different oxidation states have derived by oxidizing or reducing the already crystallized protein in the opposite state. Although there has been a report about the structures of Pf Rd (6) in its oxidized and reduced state, there is a caveat in the crystal structure of the reduced form. Those reduced crystals were obtained by adding sodium dithionite to the drops containing crystals of the oxidized form of Rd. As reported in that article, the crystal became extremely fragile upon addition of sodium dithionite, suggesting there are substantial amounts of relaxation energy generated, enough to affect the crystal lattice, thus maintaining a proper redox environment during crystallization is very important in studying the corresponding structural relaxation upon redox reaction. After a series of modifications to the crystallization methods and apparatus, we succeeded in obtaining both reduced and oxidized forms of Cp Rd crystals in the same pH and salt conditions by adjusting the reservoir and crystallization drop conditions (18). The reduced state crystals were made by adding a minimum amount of sodium dithionite ($Na_2S_2O_4$) to the reservoir. Oxidized crystals were made by instead adding an equivalent amount of sodium chloride in order to minimize the vapor pressure difference between the two crystallization processes.

Both the oxidized and reduced form of Cp Rd have five hydrogen bonds of NH···S type: two to Cys 39 Sγ from Leu 41 NH and Cys 42 NH, two to Cys 6 Sγ from Val 8 NH and Cys 9 NH, and one to Cys 9 Sγ from Tyr 11 NH. The distances between Cys 42 Sγ and Val 44 NH in both oxidized (3.72 Å) and reduced (3.84 Å) forms of Cp Rd are probably too long for a strong hydrogen bond.

Reduction of Cp Rd is accompanied by an increase in the four iron-sulfur bond lengths by an average of 0.10 Å (SD=0.03Å) consistently in all four Fe-S bonds. The degree of change in the FeS bond length found here (0.10 Å) is consistent with a study of the bis (*o*-xylyl-α,α-dithiolato) ferrate rubredoxin analog (16) and high-potential iron protein (HiPIP) (5) in which the average Fe-S bond length increased by 0.09 Å and 0.1 Å respectively, although the latter structure is at a lower resolution. This expansion of the FeS bonds has been viewed in terms of greater antibonding character in the reduced state by the unpaired electrons (5). There is also a decrease in the average NH···S hydrogen bond distance by 0.08 Å (SD=0.05Å) upon reduction consistently in all five NH···S bonds. The contraction of these NH···S bonds would help stabilize the negative charge introduced mainly onto the sulfurs upon reduction.

In addition to the structural changes of the Fe-S cluster, there is another structural change that implicates the side chain of Leu 41 in the electron transport mechanism. Leu 41 is adjacent to the Cys 42 ligand of the redox site and is found at the surface of the protein. In the reduced structure, the side chain of Leu 41 adopts two different conformations, which refine with 60% and 40% relative occupancy. However, in the oxidized structures, this side chain clearly has a single conformation similar to the 60% occupancy conformation in the reduced state.

Interestingly, the two conformations of Leu 41 in the reduced state lead to very different water structure at the redox site. In the 40% occupancy conformation of Leu 41, there is a water molecule in hydrogen bonding distance of Cys 9 Sγ and a distinct ordering of a series of water molecules following it (Fig. 3). Therefore, one conformation (40% occupancy) of residue 41 in reduced Cp Rd allows the penetration of water molecules, which, in turn, allows the formation of a string of water molecules attached to the Cys 9 Sγ. These results clearly show that the reduced form shows increased amounts of hydration around the redox site.

The two conformations also lead to very different electrostatic potential surfaces. In the oxidized state, Sγ of Cys 42, which does not have any hydrogen bonds to it from any backbone amides, is the most solvent exposed atom of the Fe-S cluster. On the other hand, in the reduced

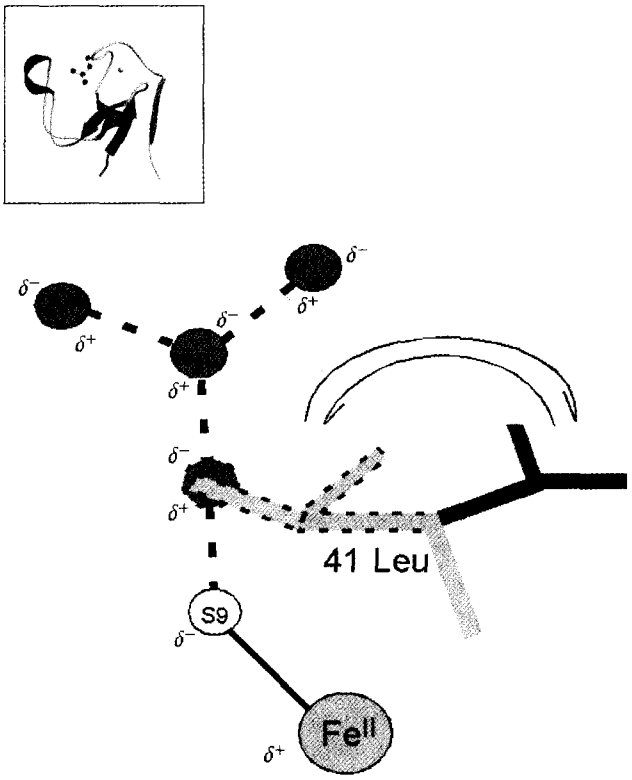

Fig. 3. Top: Rd backbone showing the position of residue Val41. Bottom: Possible redox gate mechanism based on the observed structure. In the reduced form, there are two different conformations of Leu 41 side chain. Upon reduction and consequent opening of the gate, Cys 9 S exposes its electromagnetic surface to the solvent, and this extra electronegative potential hole attracts the string of water molecules.

state, the opening of the Leu 41 gate leads to an extra electronegative potential hole around the Cys 9 Sγ on the surface of the protein.

The difference in the water structure near the redox site in the oxidized versus reduced states will obviously affect the reduction potential. The presence of a polar water molecule near the redox site in the reduced state will greatly enhance the affinity of the site for an electron by making the electrostatic environment more favorable, thus increasing the reduction potential over the case where a water molecule is not present. Recent molecular dynamics (MD) studies of Pf Rd and Cp Rd revealed significant differences in the movement of the side chain at positions 8 and 41 upon an oxidation-reduction reaction (25, 26) that are consistent with the crystal data.

Conclusion

Despite the rapidly growing number of structural information and redox potentials for a given type of redox sites, the structural origins of the enormous diversity of the redox potentials for these proteins remain unclear and quantitative predictions are still not possible. Understanding the structural origins that lead to the differences in reduction potentials is crucial to understand how the electron transfer proteins can function in such diverse roles. Moreover, an increasing number of biosynthetic pathways have been found to involve redox proteins. The information gained, therefore, can be immediately utilized in tuning bioengineering applications based on these chemical reactions.

Based on currently available information, it is likely there are local contributions from the 1) backbone, 2) polar side chain, 3) the number of hydrogen bonds to the redox center and 4) solvent near the redox site that tune the redox potential of the protein. All these properties participate in setting the value of the reduction potential, but establishing if one, or a few, of them dominates still relies on experimental work (15).

References

1. Adman, E.T., L.C. Sieker, and L.H. Jensen. 1991. Structure of rubredoxin from *Desulfovibrio vulgaris* at 1.5 Å resolution. *J. Mol. Biol.* 217, 337-352.
2. Beinert, H., R.H. Holm, and E. Munck. 1997. Iron-sulfur clusters: nature's modular, multipurpose structures. *Science* 277, 653-659.
3. Bouton, C. 1999. Nitrosative and oxidative modulation of iron regulatory proteins. *Cell. Mol. Life. Sci.* 55, 1043-1053.
4. Cammack, R. 1992. Iron-sulfur cluster in enzymes: Themes and variations. *Adv. Inorg. Chem.* 38, 281-322.
5. Carter, C.W., J. Kraut, Jr., S.R. Freer, and R.A. Alden. 1974. Comparison of oxidation-reduction site geometries in oxidized and reduced *Chromatium* high potential iron protein. *J. Biol. Chem.* 249, 6339-6346.
6. Day, M.W., B.T. Hsu, T.L. Joshua, J.B. Park, Z.H. Zhou, M.W. Adams, and D.C. Rees. 1992. X-ray crystal structures of the oxidized and reduced forms of the rubredoxin from the marine hyperthermophilic archaebacterium *Pyrococcus furiosus*. *Protein Sci.* 1, 1494-1507.
7. Eggink, G., H. Engel, G. Vriend, P. Terpstra, and B. Witholt. 1990. Rubredoxin reductase of *Pseudomonas oleovorans*. Structural relationship to other flavoprotein oxidoreductases based on one NAD and two FAD fingerprints. *J. Mol. Biol.* 212, 135-142.
8. Eidsness, M.K., A.E. Burden, K.A. Rchie, D.M. Kurtz, Jr., R.A. Scott, E.T. Smith, T. Ichiye, B. Beard, T. Min, and C. Kang. 1999. Modulation of the redox potential of the Fe(SCys)$_4$ site in rubredoxin by the orientation of a peptide dipole. *Biochemistry* 38, 14803-14809.
9. Farid, R.S., C.C. Moser, and P.L. Dutton. 1993. Electron transfer in proteins. *Curr. Op. Struc. Biol.* 3, 225-233.
10. Gomes, C.M., G. Silva, S. Oliveira, J. LeGall, M.Y. Liu, A.V. Xavier, C. Rodrigues-Pousada, and M. Teixeira. 1997. Studies on the redox centers of the terminal oxidase from *Desulfovibrio gigas* and evidence for its interaction with rubredoxin. *J. Biol. Chem.* 272, 22502-22508.
11. Gray, H.B. and W.R. Ellis, Jr. 1994. Electron transfer. p315-363. *In* I. Bertini et al (ed), University Science Books. Sausilito, CA.
12. Gray, H.B. and J.R. Winkler. 1996. Electron transfer in pro-

teins. *Ann. Rev. Biochem.* 65, 537-561.
13. Jenney, F.E., M.F.J.M Verhagen, and M.W.W. Adams. 1999. Anaerobic Microbes: Oxygen detoxification without superoxide dismutase. *Science* 286, 306-309.
14. Johnson, M.K. 1998. Iron-sulfur proteins: new roles for old clusters. *Curr. Opin. Chem. Biol.* 2, 173-181.
15. Kummerle, R., H. Zhuang-Jackson, J. Gaillard, and J.M. Moulis. 1997. Site-Directed Mutagenesis of Rubredoxin Reveals the Molecular Basis of Its Electron Transfer Properties. *Biochemistry* 36, 15983-15991.
16. Lane, R.W., J.A. Ibers, R.B. Frankel, G.C. Papaefthymiou, and R.H. Holm. 1977. Synthetic analogues of the active sites of iron-sulfur proteins. 14. Synthesis, properties, and structures of bis (*o*-xylyl-a,a'-dithiolato) ferrate(II,III) anions, analogues of oxidized and reduced rubredoxin sites. *J. Am. Chem. Soc.* 99, 84-98.
17. Marcus, R.A. and N. Sutin. 1985. Electron transfers in chemistry and biology. *Biochim. Biophys. Acta.* 811, 265-322.
18. Min, T., C. Ergenacan, M. Eidness, T. Ichiye, and C. Kang. 2001. Mechanism of the oxidation and reduction reaction in rubredoxin. *Protein Sci.* 10, 613-621.
19. Moser, C.C., J.M. Keske, K. Warncke, R.S. Farid, and P.L. Dutton. 1992. Nature of biological electron transfer. *Nature* 355, 796-802.
20. Noodleman, L., J.G. Norman, Jr., J.H. Osborne, A. Aizman, and D.A. Case. 1985. Models for ferodoxins: Electronic structures of iron-sulfur clusters with one, two and four iron atoms. *J. Am. Chem. Soc.* 197, 3418-3426.
21. Santos, H., P. Fareleira, A.V. Xavier, L. Chen, M.Y. Liu, and J. LeGall. 1993. Aerobic metabolism of carbon reserves by the obligate anaerobe *Desulfovibrio gigas*. *Biochem. Biophys. Res. Commun.* 195, 551-557.
22. Seki, S., A. Ikeda, and M. Ishimoto. 1988. Rubredoxin as an intermediary electron carrier for nitrate reduction by NAD(P)H in *Clostridium perfringens*. *J. Biochem. (Tokyo)* 103, 583-584.
23. Seki, Y., S. Seki, M. Satch, A. Ikeda, and M. Ishimoto. 1989. Rubredoxin from *Clostridium perfringens*: Complete amino acid sequence and participation in nitrate reduction. *J. Biochem. (Tokyo)* 106, 336-341.
24. Swartz, P.D., B.W. Beck, and T. Ichiye. 1996. Structural origins of redox potential in iron-sulfur proteins: Electrostatic potentials of crystal structures. *Biophys. J.* 71, 2958-2969.
25. Swartz, P.D. and T. Ichiye. 1996. Temperature dependence of the redox potential of rubredoxin from *Pyrococcus furiosus:* a molecular dynamics study. *Biochemistry* 35, 13772-13779.
26. Yelle, R.B., N.S. Park, and T. Ichiye. 1995. Molecular dynamics simulations of rubredoxin from *Clostridium pasteurianum*: changes in structure and electrostatic potential during redox reactions. *Proteins* 22, 154-167.